

Laboratory Experiments of Spray Icing on Cylindrical Specimens Using Urea-doped Water

Toshihiro Ozeki¹, Satoru Adachi², Taiki Tokudome³, Akihisa Konno³

¹ Hokkaido University of Education Sapporo, Japan

² Snow and Ice Research Center, National Institute of Earth Science and Disaster Resilience, Japan

³ Kogakuin University, Japan

ozeki.toshihiro@s.hokkyodai.ac.jp, stradc@bosai.go.jp, taiki.tokudome@gmail.com, konno@researchers.jp

Abstract— Experiments were conducted on the icing characteristics of urea-doped water spray icing including brine using cylindrical specimen with different diameters of PVC pipes. The icing was milky white in color, which showed containing urea brine, similar to seawater spray icing. Since the cylindrical specimen was placed on the floor, the icing was observed to accumulate at the bottom of the specimen. In the case of the test with high wind velocity, the droplets were observed to freeze while flowing downstream in a striated pattern. There was no significant difference in the amount of icing per unit area on the entire cylindrical specimen in the five tests with different test conditions. On the other hand, the increasing rate of cross-sectional area of ice accretion, which was obtained from graphic data analysis, was greater for the 520 mm diameter cylinder and smaller for the 165 mm cylinder.

Keywords— Spray icing, Urea-doped water, Marine icing, Laboratory experiment

I. INTRODUCTION

In recent years, the summer conditions of the Arctic Ocean have been changing year by year, and as ice concentrations weaken in summer, the use of the Northern Sea Route is expected to increase. In the future, it is expected that the number of vessels with lower ice class will increase, and heavy marine icing will be one of the most important factors to evaluate the operational safety of the Arctic shipping routes.

Several studies have investigated the physical properties of sea spray ice. Ono [1] measured the weights of ice and brine as well as the density, salinity, and growth rate of spray ice on ships. Makkonen [2] developed a theoretical model of salt entrapment in spray ice. He assumed an analogy with sponginess of fresh water ice in wet growth. Ryerson and Gow [3] studied the microstructural features of spray ice on ships and confirmed the existence of a channelized network of brine. Ozeki *et al.* [4] designed an MRI system to measure the 3D microstructures of sea spray ice. A channelized network of brine was confirmed in natural sea spray ice samples.

Numerous researchers estimated sea-water spray icing. Lozowski *et al.* [5] reviewed computer simulations of marine ice accretion and discussed the U. S. Coast Guard's Cutter Midgett model and a three-dimensional time-dependent vessel-icing model. Kulyakhtin and Tsarau [6] applied a time-dependence model, MARICE, to the prediction of marine icing. MARICE calculated the turbulent airflow, trajectories of the droplets around the complete geometry of the structure, and heat transfer from the structure. Deghani *et al.* [7][8] studied the water breakup phenomena of wave impact sea spray, and developed a three-dimensional model for calculating the movement of a cloud of wave-impact sea spray over a Medium-sized Fishing Vessel (MFV). The results of

spray impingement on the front side of the superstructure showed that 70 % of the droplets are smaller than 2 mm and 30 % are between 2 and 4 mm.

Practical icing effects on ships have been evaluated based on a relatively simple equation [9] as following,

$$PR = \frac{V_a(T_f - T_a)}{1 + 0.4(T_w - T_f)} \quad (1)$$

where PR is the predictor relating to icing rate, T_f is freezing point of seawater [$^{\circ}\text{C}$], T_a is air temperature [$^{\circ}\text{C}$], T_w is sea temperature [$^{\circ}\text{C}$], V_a is wind speed [m s^{-1}]. The factor used to estimate the severity of potential spray icing is derived from a simplified heat balance of the icing surface, which do not consider the characteristics of individual ships or the availability of anti-icing measures.

Although the PR values are useful for evaluating the safety of icing during navigation, more information is needed to use them in ship design and operational planning. In this study,

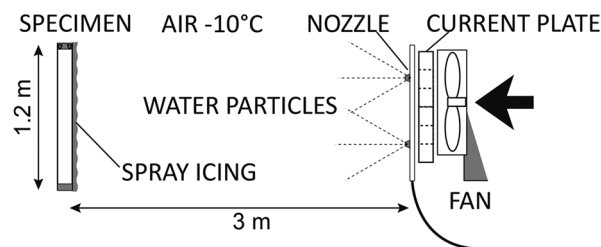


Fig. 1 A schematic view of experimental setting.



Fig. 2 An ice tank (20 m × 6 m × 1.8 m) at JMU Technical Research Center.

TABLE 1. SPECIMEN DIAMETER AND SPRAY PARTICLE DIAMETER

Diameter [mm]	240 μm droplets		120 μm droplets	
	10 m/s	7.5 m/s	10 m/s	7.5 m/s
520	#A52	#B52	#D52	#C52
165	#A16	#B16	#D16	#C16
60	#A6	#B6	#D6	#C6

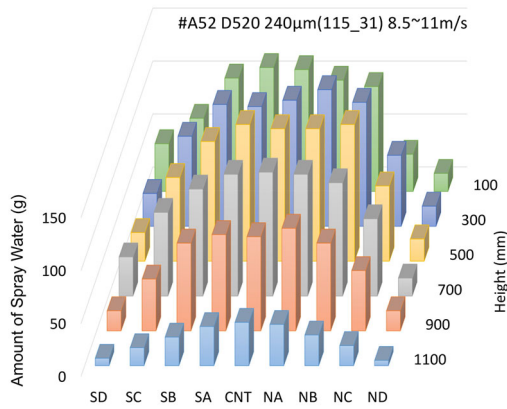


Fig. 3 Spray distribution measured on cylinders of 520 mm diameter. Wind speed: 10 m/s, droplet size: 240 μm (#A52).

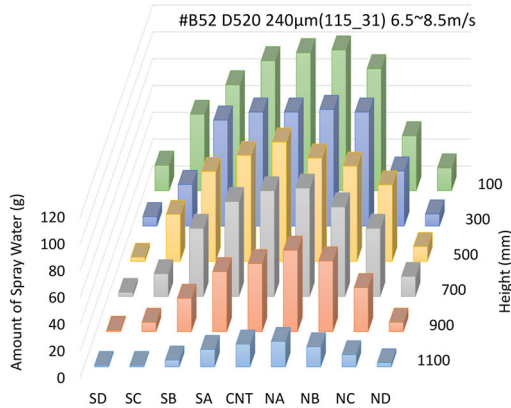


Fig. 4 Spray distribution measured on cylinders of 520 mm diameter. Wind speed: 7.5 m/s, droplet size: 240 μm (#B52).

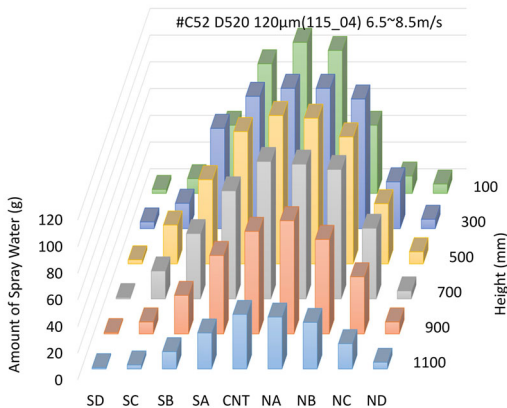


Fig. 5 Spray distribution measured on cylinders of 520 mm diameter. Wind speed: 7.5 m/s, droplet size: 120 μm (#C52).

urea-doped spray icing experiments were conducted using simple-shaped test pieces that resembles a member of a ship's superstructure with the goal of predicting the amount of icing on individual vessels.

II. EQUIPMENT FOR SPRAY ICING EXPERIMENTS

In this study, an experimental apparatus (Fig. 1) was set up on an ice tank (20 m in length \times 6 m in width \times 1.8 m in depth: Fig. 2) at the Technical Research Center of Japan Marine United Inc. Since the use of sodium chloride water was forbidden in this ship model basin, and model ice was made with urea-doped water, wet ice was grown by spraying urea-doped water with a concentration of about 20 ‰ to conduct experiments on the icing characteristics of brine-containing ice.

Two fan-shaped nozzles (VE115-31, Ikeuchi) or four fan-shaped nozzles (VP115-04, Ikeuchi) were installed on both sides of the fan, so that the sprayed water droplets were supplied to the cylindrical test specimen by the wind. The spray particle size distribution was measured by the spray particle counter SPC. Since the major grain size of VE115-31 was about 240 μm and that of VP115-04 was about 120 μm , the former is referred to as small particles and the latter as fine particles in this study. The room temperature in the cold room was controlled at approximately -10°C .

For the first effort, cylindrical specimens were selected to resemble cylindrical members found on ships, such as columns, poles and capstans. Cylindrical PVC models with diameters of 520 mm, 165 mm or 60 mm and a height of 1.2 m was fixed on a dolly (Fig. 2). The distance of the specimen from the spray nozzle was 3 m. Prior to each icing experiment, the distribution of wind velocity around the specimen and the distribution of the impinging spray amount were measured separately (Fig. 3 – 5).

III. EXPERIMENTAL RESULTS

A. Observation of Ice Shape and Amount of Icing

The icing tests were conducted 12 times with different specimen diameters, wind speeds and spray particle sizes (Table 1). In this experiment, the wind speed was approximately 10 m/s or 7.5 m/s near the center of the specimen. The spraying was supplied continuously. The tests were conducted for 30 minutes each (20 minutes for the #A52 test only), and the ice weight and salinity were measured at the end of each test at each one sixth height.

In this study, all experiments were conducted at a room temperature of -10°C . The freezing temperature of 20‰ urea-doped water is -0.6°C . The urea-doped water was supplied by a pump from the ice tank. The surface of the tank was often covered with a thin ice layer during the experiments, and the spray temperature was close to the freezing temperature, although the hose and nozzles of the spray system were heated to prevent freezing. Wind speeds were approximately 10 m/s and 7.5 m/s, respectively. Therefore, assuming that the denominator in equation (1) is about 1, $PR = 94$ for the 10 m/s experiments and $PR = 66$ for the 7.5 m/s experiments. These values correspond to Extreme (Icing rate > 4.0 cm/h) and Heavy (Icing rate 2.0 – 4.0 cm/h) in Icing Class [9], respectively.

In this paper, we focus on five tests (#A52, #B52, #C52, #B16, #C16: Fig. 6 and Fig. 8), and focus on the initial

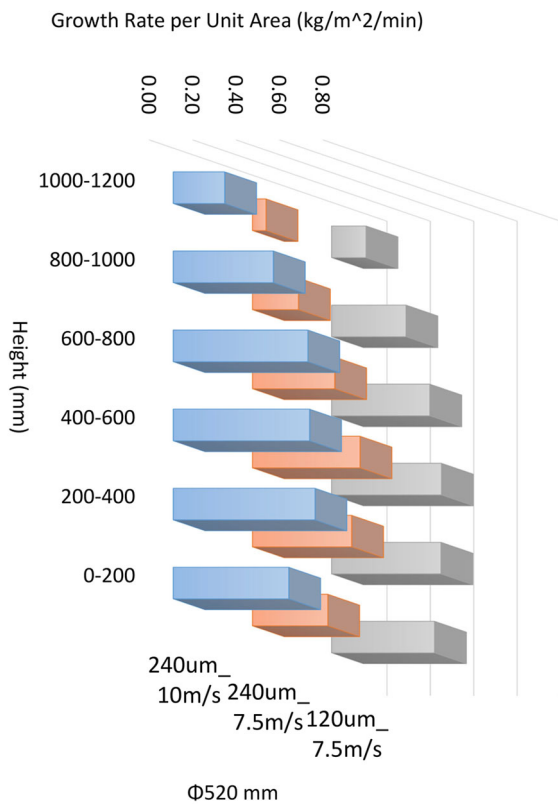


Fig. 6 Ice weight measured at the end of each test at each one sixth height of cylinders of 520 mm diameter.

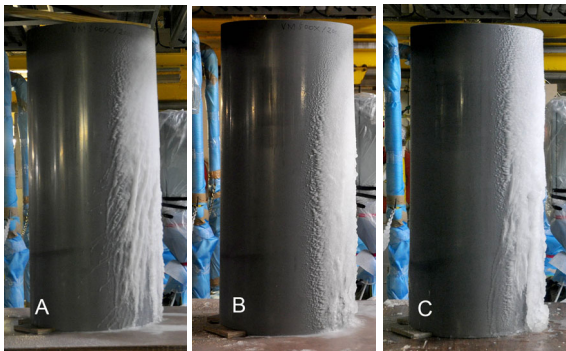


Fig. 7 Examples of icing on a PVC cylinder of 520 mm diameter. A: #A52, B: #B52, C: #C52.

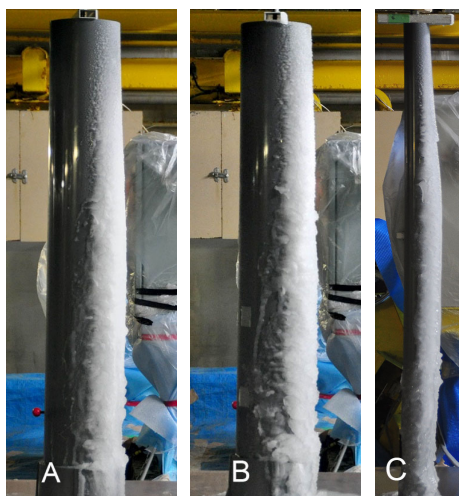


Fig. 9 Examples of icing on a PVC cylinder of 165 mm and 60 mm diameter. A: #B16, B: #C16, C: #C6.

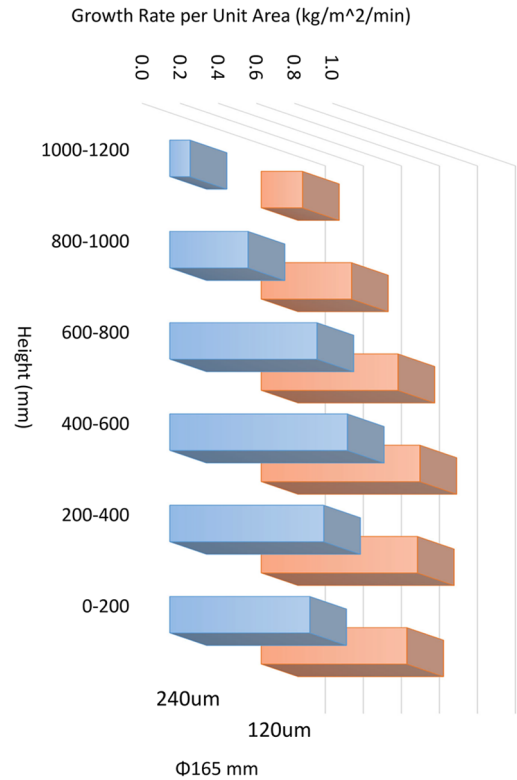


Fig. 8 Ice weight measured at the end of each test at each one sixth height of cylinders of 165 mm diameter.

TABLE 2. AMOUNT OF SPRAY WATER IMPINGING ON THE SPECIMEN AND AMOUNT OF ICING

	A: Spraying [kg m ⁻² min ⁻¹]	B: Ice Accretion [kg m ⁻² min ⁻¹]	B/A
#A52	6.24	3.01	0.48
#B52	3.86	1.88	0.49
#B16	6.06	3.43	0.57
#C52	5.08	2.35	0.46
#C16	7.09	3.48	0.49

growth of ice, growth rate, shape and amount of ice accretion. Fig. 7 and Fig. 9 show examples of ice accretion on a cylindrical PVC specimen with a diameter of 520 mm, 165 mm and 60 mm. There were differences in the shape of the ice formed on the specimens in the early stages of growth. In the initial stages, part of the water froze into spongy ice as it flowed down the PVC surface, and the surface gradually began to be covered by sheet-like ice. In the experiments of spraying small droplets (about 120 μm), especially in the large diameter cylinder (Φ520), part of the sheet ice often exfoliated and slid down the surface as slush in the early stages of growth, and eventually, the ice piled up on the lower end (Fig. 7C). On the other hand, in the experiment with a wind speed of 10 m/s (Fig. 7A), the droplets were observed to freeze while flowing downstream in stripes. The wet growth of spray icing was similar to the experimental results using sodium chloride water [10]. The shape and milky white in color of the spray ice formed in this study was similar to that of ice samples collected in actual ship icing. The most important point was that the spray ice made of urea-doped water had brine channels in it similar to that of sea-water spray ice. Thus, brine-containing spray icing can be produced in urea-doped water.

Fig. 6 and Fig. 8 show that ice accretion grew significantly from the center of the cylinder to the lower half. This is due to the smaller amount of spray impinging on the top of the cylinder as seen in Fig. 3, 4, 5, as well as unfrozen urea water supplied to the lower part of the cylinder and freezing. Additionally, as mentioned above, this is also due to the fact that the slush froze at the bottom of the cylinder.

Table 2 shows the amount of spray water impinging on the specimen per unit time and unit area (A), and the amount of icing per unit time and unit area (B); the projected area of the side surface of the specimen was used to calculate per unit area. Since the wind speed, projected area, and droplet particle size of each test were different, a direct comparison of the above values does not reveal a relationship. Therefore, the ratio B/A, which represents the freezing rate relative to the impinging urea-doped water, was calculated. In each experiment, about half of the impinging spray was frozen under these conditions, and there was no significant difference in the amount of ice formed on the entire specimen per unit area. Thus, in the five tests presented here, it was found that the diameter of the specimen had a small effect on the amount of ice per unit area.

B. Graphic Data Processing

Projection area of ice accretion was obtained from graphic data set of each experiment. The method for detecting ice accretion areas from interval photographs of specimens has



Fig. 10 Cross-section area of the spray ice. Left: a PVC cylinder of 520mm diameter (#C52), Right: difference between the trimming area including the spray ice and the projected area of specimen.

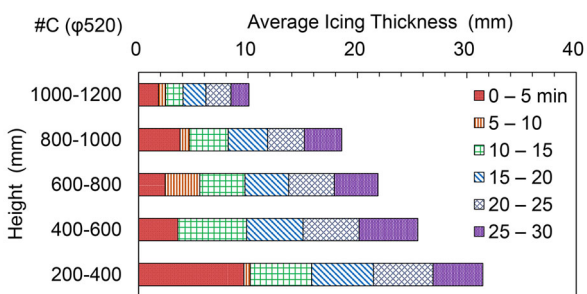


Fig. 11 Thickness of ice accretion every 5 minutes at every 20 cm height on a PVC cylinder of 520mm diameter (#C52).

been used for the marine icing on ships [11] and the seawater spray icing on breakwater light-beacons [12]. In this study, the photographs were taken every minute from left side, and cropped to leave only the subjects that include ice accretion and the specimen. The cross-section area of the spray ice was obtained from the difference between the projected area of the trimming area including the spray ice and the projected area of specimen (Fig. 10).

Fig. 11 shows the cross-sectional area of ice accretion every 5 minutes at every 20 cm height in test #C52, and converted to the average thickness of ice accretion every 5 minutes at each height. The projected area of 0-200 mm included ice piled up from the floor and was excluded from the analysis

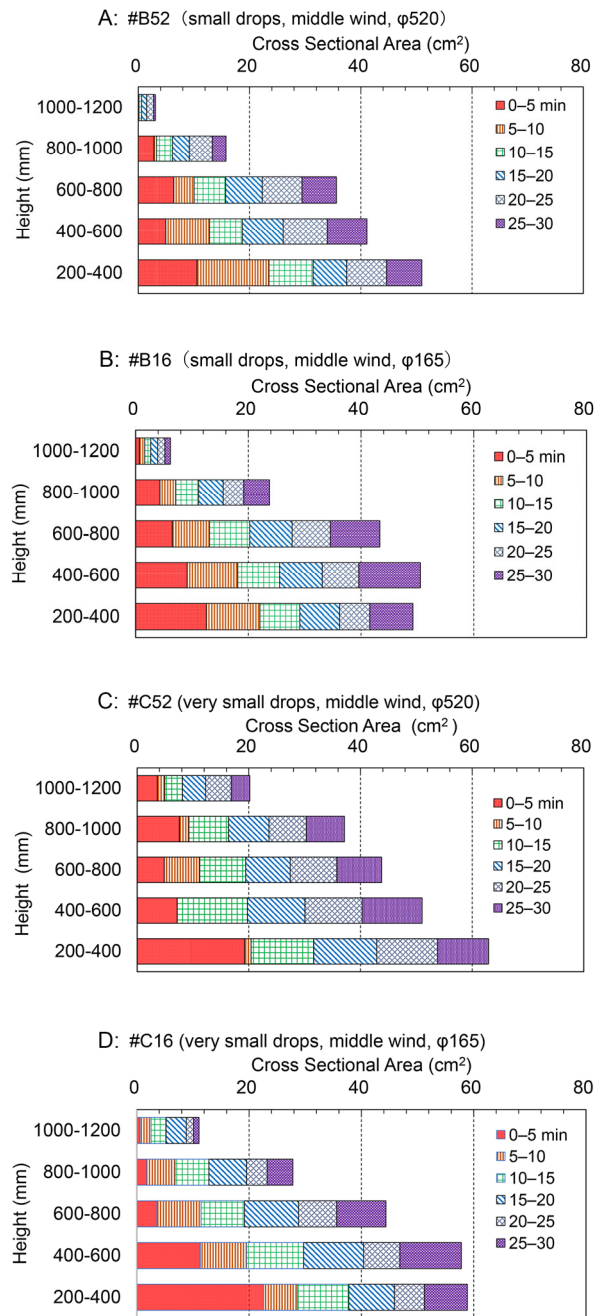


Fig. 12 Comparison of cross-sectional area of ice accretion every 5 minutes. A: #B52, B: #B16, C: #C52, D: #C16.

because it was difficult to separate ice accretion from ice on the floor. Focusing on the amount of growth during the first 5 minutes, the growth near the center of the cylinder (600-800 mm) was small. On the other hand, no growth was recorded at 400-600 mm in 5-10 min. This is because the sheet icing exfoliated and slide off. However, the growth became stable after that, and a distribution of thicker icing in the lower layers and thinner icing in the upper layers was formed after 30 minutes.

Fig. 12 shows four graphs of the cross-sectional area of ice accretion every 5 minutes for tests #B52 (Fig. 12A), #B16 (Fig. 12B), #C52 (Fig. 12C), and #C16 (Fig. 12D) at heights of every 20 cm. In this figure, the cross-sectional area (cm²), rather than the thickness of ice accretion (mm), was presented for the purpose of comparison of each test. In the initial stage, there were differences in the vertical distribution of icing area depending on the diameter of the cylinder: for the specimens with $\Phi 520$ (#B52, #C52), the area decreased once at 400-600 mm, while for the specimens with $\Phi 165$ (#B16, #C16), the area monotonically increased toward the lower layers.

However, after 30 minutes, the icing area in all specimens reached the distribution with thicker ice accretion in the lower layers and thinner ice accretion in the upper layers.

To compare the growth rate of icing on each tests in Fig. 12, the cross-sectional area of ice accretion was calculated every 5 minutes and plotted in Fig. 13. The dashed lines are regression lines, respectively; the correlation coefficients r were 1.00 (#B52), 1.00 (#B16), 0.99 (#C52), and 1.00 (#C16), all showing strong positive correlation. On the other hand, the fine particles (#C: major grain size about 120 μm) tended to increase at a higher rate, but it is necessary to distinguish whether this was due to the contribution of particle size or the amount of impinging spray per unit time. The cross-sectional area of ice accretion divided by the spray rate ($\text{kg m}^{-2} \text{min}^{-1}$) for each test was plotted in Fig. 14. The increasing rate was greater for the 520 mm diameter cylinder and smaller for the 165 mm cylinder. For the same diameter, the increasing rate for fine particles (#C) was slightly greater than that for small particles (#B).

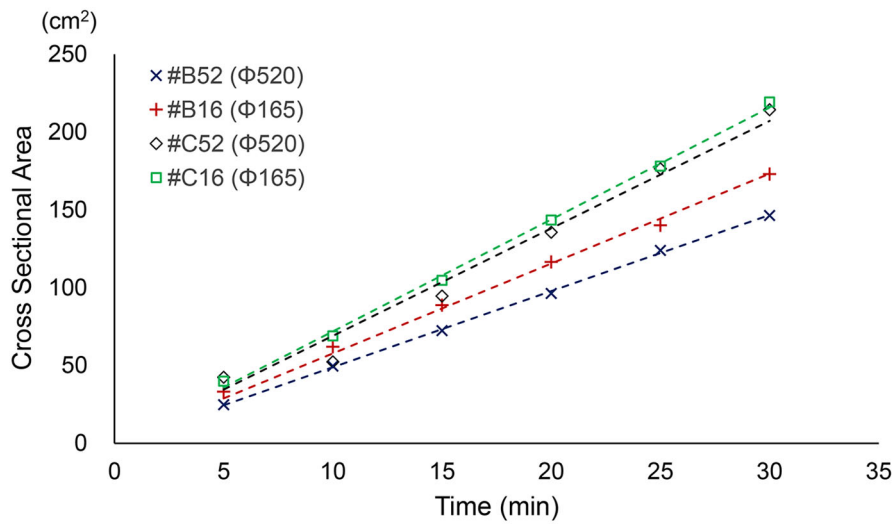


Fig. 13 Time series of cross-sectional area of ice accretion every 5 minutes.

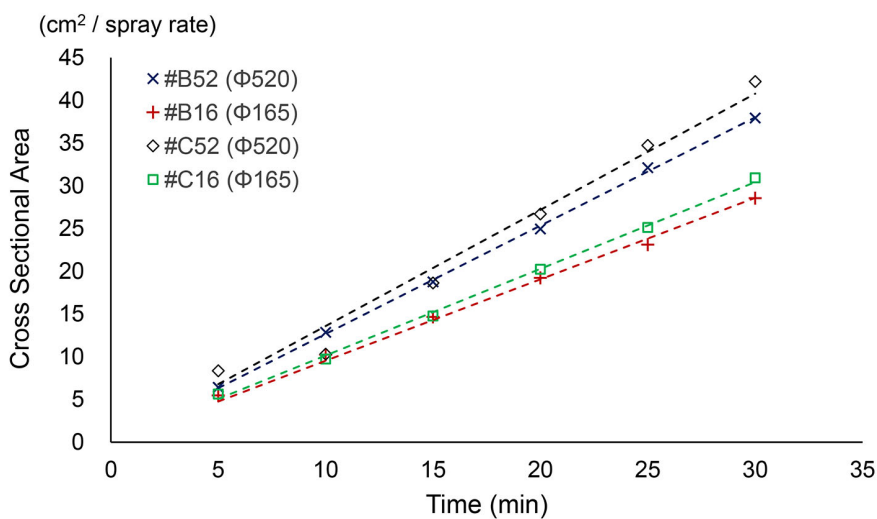


Fig. 14 Time series of cross-sectional area of ice accretion divided by the spray rate ($\text{kg m}^{-2} \text{min}^{-1}$) every 5 minutes.

Since these results were obtained for a two-dimensional area, further work will be needed to analyse the relationship to the weight of icing. Furthermore, the analysis did not capture changes in weight due to brine drainage, which is a characteristic feature of seawater splay icing. Further work will be required to estimate the icing weight over several hours.

IV. CONCLUSIONS

To obtain data that will contribute to the improvement of the *PR* equation, urea-doped spray icing experiments were conducted using simple-shaped test pieces. The icing tests were conducted 12 times with different specimen diameters, wind speeds and spray particle sizes. The ice weight and salinity were measured at the end of each test at each one sixth height.

The icing was milky white in color, which showed containing urea brine, similar to seawater spray icing. There was a difference in the shape of the icing depend on the wind speed. Since the cylindrical specimen was placed on the floor, the icing was observed to accumulate at the bottom of the specimen. In the case of the test with high wind velocity, the droplets were observed to freeze while flowing downstream in a striated pattern. The freezing rate relative to the impinging urea-doped water was calculated for the five tests. In each experiment, about half of the impinging spray was frozen, and there was no significant difference in the amount of ice formed on the entire specimen per unit area. The result suggested that the diameter of the specimen had a small effect on the amount of ice per unit area.

On the other hand, the increasing rate of cross-sectional area of ice accretion, which was obtained from graphic data analysis, was greater for the 520 mm diameter cylinder and smaller for the 165 mm cylinder. Since the result was obtained in a two-dimensional analysis, further work will be needed to analyse the relationship with the weight of icing.

We plan to use this experimental data to estimate the trajectory of spray particles around the hull of a ship using computational fluid dynamics (CFD) analysis to evaluate the amount of icing on the upper structure of the ship.

ACKNOWLEDGMENT

We wish to express our gratitude to Dr. T. Matsuzawa of National Maritime Research Institute, S. Mizuno, N. Nakazato and A. Maeda of JMU Technical Research Center for their support in the laboratory experiments. We also thank to T. Nunokawa, Y. Matsuda, M. Miura, K. Orime and Y. Souma of Hokkaido University of Education for their cooperation in the laboratory experiments. This work was supported by ArCS II JPMXD1420318865.

REFERENCES

- [1] N. Ono, "Studies on the ice accumulation on ships. 2. On the conditions for the formation of ice and the rate of icing," *Low Temp. Sci.*, A22, pp. 171–181, 1964. [in Japanese]
- [2] L. Makkonen, L. "Salinity and growth rate of ice formed by sea spray," *Cold Reg. Sci. Tech.*, 14, pp. 163–171, 1987.
- [3] C.C. Ryerson and A.J. Gow "Crystalline structure and physical properties of ship superstructure spray ice," *Phil. Trans. R. Soc. Lond.*, A358, pp. 2847–2871, 2000.
- [4] T. Ozeki, K. Kose, T. Haishi, S. Nakatsubo and Y. Matsuda, "Network images of drainage channels in sea spray icing by MR microscopy," *Mag. Res. Imag.*, 23, pp. 333-335, 2005.
- [5] E.P. Lozowski, K. Szilder and L. Makkonen, "Computer simulation of marine ice accretion," *Phil. Trans. R. Soc. Lond.*, A358, pp. 2811–2845, 2000.
- [6] A. Kulyakhtin and A. Tsarau, "A time-dependent model of marine icing with application of computational fluid dynamics," *Cold Reg. Sci. Tech.*, 104-105, pp. 33-44, 2014. doi.org/10.1016/j.coldregions.2014.05.001.
- [7] S.R. Dehghani, Y.S. Muzychka and G.F. Naterer, "Water breakup phenomena in wave-impact sea spray on a vessel," *Ocean Eng.*, 134, pp. 50-61, 2017. doi.org/10.1016/j.oceaneng.2017.02.013.
- [8] S.R. Dehghani, G.F. Naterer and Y.S. Muzychka, "3-D trajectory analysis of wave-impact sea spray over a marine vessel," *Cold Reg. Sci. Tech.*, 146, pp. 72-80, 2018. doi.org/10.1016/j.coldregions.2017.11.016.
- [9] J.E. Overland, "Prediction of Vessel Icing for Near-Freezing Sea Temperature," *Weather and Forecasting*, 5, pp. 62-77, 1990.
- [10] T. Ozeki, H. Shimoda, D. Wako, S. Adachi and T. Matsuzawa, "Laboratory experiments of saline water spray icing - Features of hydrophilic and hydrophobic pliable sheets," in *Proc. IWAI2013*, 5pp, 2013.
- [11] R. Gagnon, M. Sullivan, W. Pearson, W. Bruce, D. Cluett, L. Gibling and L.F. Li, "Development of a marine icing monitoring system," in *Proc. POAC2009*, 2009, 9pp.
- [12] T. Ozeki, Y. Tamate, S. Adachi, K. Izumiyama and T. Tazawa, "Field observation of sea spray icing on lighthouses and ice adhesion test of superhydrophilic pliable sheet for deicing," in *Proc. IWAI2009*, 2009, 5pp.